SosA inhibits cell division in *Staphylococcus aureus* in response to DNA damage

Martin S. Bojer[a,b], Katarzyna Wacnik[c], Peter Kjelgaard[a], Clement Gallay[d], Amy L. Bottomley[c,*], Marianne T. Cohn[a], Gunnar Lindahl[a], Dorte Frees[a], Jan-Willem Veening[d], Simon J. Foster[c] & Hanne Ingmer[a,b,#]

[a]Department of Veterinary and Animal Sciences, Faculty of Health and Medical Sciences, University of Copenhagen, Copenhagen, Denmark.

[b]Centre for Bacterial Stress Response and Persistence, University of Copenhagen, Copenhagen, Denmark.

[c]The Krebs Institute, Department of Molecular Biology and Biotechnology, University of Sheffield, Sheffield, United Kingdom.

[d]Department of Fundamental Microbiology, University of Lausanne, Lausanne, Switzerland.

[*]Present address: The ithree Institute, University of Technology Sydney, Sydney, NSW, Australia.

Short title: SosA inhibits *S. aureus* cell division

Key words: *Staphylococcus aureus*, cell division, SOS response, cell-division inhibition, SosA, CtpA, PBP1

Classification: Biological Sciences, Microbiology

[#]Corresponding author: Hanne Ingmer; Stigbøjlen 4, 1870 Frederiksberg, Denmark; Telephone: +45 2215 9518; email: hi@sund.ku.dk

Abstract

Inhibiting cell division under DNA-damaging conditions is critical for cell viability. In bacterial cells, DNA damage induces the SOS response, which inhibits cell division to prevent compounding damage while repairs are made. In the rod-shaped bacterium, *Escherichia coli,* the SOS-controlled inhibitor SulA blocks division at an early step, but in coccoid bacteria, such as the human pathogen *Staphylococcus aureus*, the link between DNA damage and cell-division inhibition remains poorly understood. To enhance our knowledge and provide unique pathways for therapeutic intervention, we studied this process in *S. aureus* and have identified and characterized an SOS-induced cell-division inhibitor, designated SosA. In contrast to cells lacking *sosA*, wildtype cells increase in size upon DNA damage due to cell-division inhibition and display a concomitant superior viability. This 77-amino-acid protein is conserved in *S. aureus*, with homologs being present among staphylococci, and we have provided evidence to support its predicted membrane localization. Functional studies showed that it does not interfere with early cell-division events, such as Z-ring formation, but rather interacts with known divisome components, particularly PBP1, at a later stage. Characterization of truncated SosA variants and mutant strains revealed that the extracellular C-terminus of SosA serves dual functions as a required component for cell-division inhibition while simultaneously controlling SosA levels by acting as a likely target for degradation by the uncharacterized membrane protease CtpA. Our findings provide important insights into the regulation of cell division in coccoid bacteria that in turn may foster development of new classes of antibiotics targeting this essential process.

Significance

Staphylococcus aureus is a clinically relevant human pathogen and model organism for cell-division studies in spherical bacteria. We show that SosA is the DNA-damage-inducible cell-division inhibitor in *S. aureus* that upon expression causes cell swelling and cessation of the cell cycle at a stage prior to division plate completion. SosA appears to function by interfering with the essential membrane-associated division protein PBP1, while being negatively regulated by the membrane protease CtpA. This report represents the first comprehensive description of an endogenous cell-division inhibition mechanism in coccoid bacteria. Uncovering the molecular details of SosA function and regulation can lead to target identification for development of valuable new antibacterials against staphylococci.

Introduction

Bacteria multiply by coordinated and essential DNA replication and cell-division events, two important biological processes that are valuable targets for antimicrobial therapy (1-4). In the event of DNA damage, the SOS response is activated and ensures that cell division is delayed until the DNA is repaired. The SOS regulon is controlled by the conserved LexA repressor, which is inactivated in response to RecA, a sensor of DNA damage at stalled replication forks, binding to single-stranded DNA (5-7). The SOS response has been mostly studied in *Escherichia coli*, a gram-negative rod-shaped bacterium. Among the LexA-regulated genes in *E. coli* is *sulA*, which encodes a cell-division inhibitor. This inhibitor suppresses division by binding to FtsZ, which acts as a scaffold for the assembly of cell-division components at the division site (4, 8-13). In rod-shaped

bacteria, inhibiting cell division leads to filamentation as a consequence of lateral peptidoglycan synthesis. This phenotype is also observed in *E. coli* mutants lacking the Lon protease for which SulA is a substrate, further substantiating the role of SulA in cell-division inhibition and filamentation (14, 15).

SulA is poorly conserved in species outside Enterobacteriaceae and the α-proteobacterium *Caulobacter crescentus* encodes another SOS-induced cell-division inhibitor SidA that does not show homology to SulA. In contrast to cytosolic SulA, SidA is a membrane-anchored, small protein, which does not interact with FtsZ but rather with later cell-division proteins (16). Hence, it appears that fundamental differences exist as to how different bacteria orchestrate regulated cell-division inhibition. For gram-positive, spherical cells such as *Staphylococcus aureus*, however, little is known of how SOS induction is coupled to cell division nor have specific posttranslational mechanisms for the negative regulation of cell-division inhibition been identified in gram-positive species at present.

S. aureus is a serious gram-positive human pathogen, notorious for being implicated in a wide range of infections and for being able to acquire resistance towards important antibiotic classes. It originally received its name from the grape-like clusters of coccoid cells that result from the unique cell-division process that occurs in three consecutive orthogonal planes (17-19). In this organism, we and others have previously identified *lexA* and noted an open reading frame (designated *sosA*) that was divergently transcribed from *lexA* and controlled by the LexA repressor and the SOS response (20-23). The location of *sosA* adjacent to *lexA* indicated that it might encode a cell-division inhibitor, as similar gene synteny has been observed for SOS-induced, cell-division inhibitors encoded by gram-positive, rod-shaped bacteria, namely *Bacillus subtilis* (24), *Bacillus*

megaterium (25), *Listeria monocytogenes* (26, 27), *Mycobacterium tuberculosis* (28), and *Corynebacterium glutamicum* (29) (Fig. 1*A*). The cell-division inhibitors of these organisms display no similarity to SulA, and within the group they generally show little homology with the exceptions of YneA from *L. monocytogenes* and ChiZ from *M. tuberculosis* (28) that resemble *B. subtilis* YneA. Commonly, however, they have a single membrane spanning segment, a predicted extracellular C-terminus and, except for DivS from *C. glutamicum*, a LysM domain, which is a ubiquitous peptidoglycan binding motif (30, 31), suggesting that membrane and/or cell-wall localization is a common feature characterizing gram-positive cell-division inhibitors.

The fundamental processes of staphylococcal cell division have been studied spatiotemporally using super-resolution microscopy techniques (18, 32), and recent efforts combining genetic approaches have unveiled the molecular mechanism in unprecedented detail (33, 34). Here, we demonstrate that *sosA* encodes the SOS-inducible cell-division inhibitor in *S. aureus* and document its impact on cell division following treatment with DNA damaging agents. Moreover, we identify a possible mechanism for the proteolytic control of endogenous cell-division inhibition. Thus, we further our insight into these basic biological phenomena, which could lead to the development of new antimicrobials targeting the cell-division machinery in *S. aureus*.

Results

Conservation of *sosA* in staphylococci. In *S. aureus*, the open reading frame located adjacent to *lexA* (divergently transcribed) was named *sosA* and hypothesized to encode an inhibitor of cell division (Fig. 1*A*) (22). To determine the role of this gene in staphylococci and identify important

characteristics of the protein to investigate further, homology studies were conducted comparing that of *S. aureus* to a number of other species. The 77-amino-acid-long product has homology and 25-60% amino-acid identity to proteins encoded by genes occupying the same chromosomal location in a range of staphylococci (Fig. 1*B* and *SI Appendix*, Fig. S1), while showing no clear homology to the known gram-positive cell-division inhibitors. Of note, the C-terminal part of SosA lacks a LysM domain, which is present in the cell-division inhibitors YneA and ChiZ (35, 36). The N-terminal half of SosA includes a putative transmembrane (TM) domain, and the C-terminal part is predicted to be located extracellularly (TOPCONS server [37]). Among the different staphylococcal species, a highly conserved sequence is located just C-terminally of the predicted TM domain and, although less striking, some conservation also seems to exist in the extreme C-terminus (Fig. 1*B*).

Genotoxic stress inhibits cell division in an SosA-dependent manner. To analyze whether SosA serves as an SOS-induced cell-division inhibitor, we deleted *sosA* from 8325-4, the common laboratory *S. aureus* strain, and JE2, a derivative of the clinically relevant USA300 lineage. Growth and survival of these mutants was monitored upon challenge with a lethal concentration of the DNA damaging agent Mitomycin C (MMC). Within a two-hour-long MMC killing experiment, wildtype cells with a functioning SosA protein showed a 10-100-fold higher survival rate than the mutant cells lacking SosA at each time point, whereas the optical densities of both cell type cultures were comparable (Fig. 2*A*). Flow cytometry measurements of arbitrary cell size distributions revealed that treatment with MMC led to a three- and six-fold increase in forward light scatter (FSC-A) values in 8325-4 and JE2, respectively, while the cell size distribution of the mutants lacking *sosA* remained essentially constant (Fig. 2*B*). The constant cell size of the mutants lacking *sosA* during DNA damage could imply that these cells, in contrast to wildtype cells, continue dividing. Indeed, this striking phenotype was confirmed by time-lapse microscopy, where

wildtype cells increased in size over time, occasionally growing so large that lysis occurred, while the size of the mutant cells lacking *sosA* stayed the same and cell division continued (Fig. 2*C* and Movie S1). The phenotypes of the 8325-4 *sosA* mutant were abrogated in a strain complemented with a chromosomal copy of *sosA* expressed from its native promoter (*SI Appendix*, Fig. S2). Thus, the SosA protein seems to prevent or delay cell division, maintaining viability of *S. aureus* under DNA damaging conditions, and as a consequence of continued peptidoglycan synthesis causing cell sizes to increase.

SosA inhibits cell division. If SosA is indeed a cell-division inhibitor in *S. aureus*, it can be predicted that overexpression of the protein should be sufficient to inhibit growth under DNA non-damaging conditions. Hence, we expressed *sosA* episomally from an anhydrotetracycline (AHT)-inducible promoter and found that while the control vector does not affect cell viability in either the presence or absence of the inducer, the plating efficiency of cells with the plasmid for *sosA* overexpression was markedly compromised under inducing conditions (Fig. 3*A*). When grown in liquid culture and compared to the control, there was a 2-3-fold increase in forward light scatter values, showing that the size of the *sosA*-expressing cells increased (Fig. 3*B*). Microscopy observations over time confirmed the slight increase in cell size and the reduction in the overall number of cells upon SosA overproduction (Fig. 3*C* and Movie S2). Interestingly, contrary to what was observed upon sustained DNA-damaging conditions (Fig. 2*B*), we found that ectopic induction of SosA caused only a transient increase in cell size (compare time points 45 and 90 min to 135 min in Fig. 3*B*), indicating the existence of a negative regulatory mechanism.

SosA is a late-stage cell-division inhibitor. To pinpoint at which step of the cell-division process the SosA-mediated inhibition is taking place, we employed fluorescence microscopy to monitor

the cellular localization of FtsZ and EzrA, crucial cell-division proteins in *S. aureus*, upon the induction of SosA overproduction. Neither the *sosA* overexpression plasmid in non-inducing conditions (Fig. 4*A* and *B*) nor the control vector in non-inducing and inducing conditions (*SI Appendix*, Fig. S3*A* and *B*) changed the cell morphology and protein localization. Contrasting with the cell-division inhibitor SulA in *E. coli*, *sosA* overexpression caused cell swelling but did not affect the localization of the cell-division initiator FtsZ (Fig. 4*A*) or the placement of the membrane-bound division protein EzrA (Fig. 4*B*), which is an early recruited protein connecting the cytoplasmic division components with the peptidoglycan-synthesizing membrane-bound complex (38).

To further explore the cellular consequences of SosA-mediated cell-division inhibition, we examined the phenotypes of JE2/pSosA cells that were labeled for five minutes with HADA, marking regions of nascent peptidoglycan synthesis, and grown in the absence or presence of inducer (*SI Appendix*, Fig S3*C*). While in the absence of AHT, 47% and 23% of cells, respectively, showed a ring (incomplete septum) or line (complete septum) of nascent peptidoglycan synthesis, there was accumulation (89%) of cells with incomplete septa and a severe drop in cells with complete septa (1%) when *sosA* was overexpressed (Fig. 4*C*). Additionally, 1% of cells had an 'hourglass' shape after incubation with AHT, indicative of non-productive, premature splitting taking place prior to septum completion. Next, whole cell walls of those cells that overproduced SosA were labeled with a fluorescent NHS ester and examined by 3D-structured illumination microscopy (3D-SIM). Microscopy visualization revealed that most cells had only signs of septation — a 'piecrust' (18) (*SI Appendix*, Fig. S3*E*i) — and showed that in an hourglass-like cell, there was a gap in the septal peptidoglycan (*SI Appendix*, Fig. S3*E*ii). The fact that SosA does not affect localization of early cell-division proteins, FtsZ and EzrA, and the cell population becomes

synchronized to a particular stage of the cell cycle (phase P2 [32]) suggests that SosA does not hinder the initiation of septum formation but blocks the progression of septum completion — a phenotype similar to *S. aureus* DivIB-depleted cells (39). Although DivIB has been shown to be dispensable for FtsZ and EzrA localization to the septum and piecrust formation, its absence results in the inhibition of septum progression and completion and in the mislocalization of GpsB (39), a late cell-division protein (39, 40). Again, under non-inducing conditions, SosA did not alter cell morphology and GpsB-GFP localization (Fig. 4*D*), and the control vector did not have any effect on the presence and absence of AHT (*SI Appendix*, Fig. S3*D*). Interestingly, while causing visible cell enlargement in this reporter strain, SosA overproduction also did not impair the recruitment of GpsB to the mid-cell (Fig. 4*D*), indicating that SosA acts on (a) later cell-division component(s) than GpsB.

SosA interacts with PBP1. No direct interaction has been observed between the gram-positive cell-division inhibitors and FtsZ, the scaffold for cell-division components assembly at the division site. Though poorly characterized mechanistically, the gram-positive inhibitors may suppress cell division at later stages, potentially by interacting with FtsI/FtsQ (for *M. tuberculosis* ChiZ)(35) or via delocalization of FtsL and/or DivIC (for *B. subtilis* YneA) (41). By employing a bacterial two-hybrid system approach that reports protein-protein interactions, we sought to identify possible *in vivo* interaction candidates for SosA based on cell-division proteins from *S. aureus* (38). This analysis indicated that PBP1 (penicillin-binding protein 1) and possibly also DivIC and PBP3 are likely targets for the activity of SosA (Fig. 5*A*). PBP1, which is a homolog of *E. coli* FtsI (42), is an essential component of the divisome that, in *S. aureus*, is considered to play a role in septum formation and cell separation, with only the latter activity relying on transpeptidase (TP) functionality of the enzyme (43). If PBP1 is indeed a target for SosA, it seemed possible that

ectopic expression of *pbpA* (encoding PBP1) would mitigate the effect of concomitant *sosA* overexpression by increasing the level of target protein. Intriguingly, overproduction of PBP1 along with SosA manifested as a synergistically lethal phenotype that lead to considerable growth impairment even at low inducer concentrations, whereas the effects of SosA or PBP1 overproduction alone were negligible (Fig. 5*B*). While this does not suggest a simple titration of SosA by PBP1, wherein excess PBP1 is able to alleviate the inhibitor activity of SosA, it does support the evidence from the two-hybrid system that SosA is mechanistically linked to PBP1. To further explore this, we found that SosA was also synergistically lethal when co-expressed with a mutant variant of PBP1 lacking TP activity (*SI Appendix*, Fig. S4). This indicated that SosA works to obstruct septum formation progression and closure in *S. aureus* through an interaction with PBP1 and with a mechanism independent of the PBP1 TP activity.

The C-terminal part of SosA is functionally essential and possibly required for autoregulation.

The C-terminal part of SosA contains segments that appear highly conserved in staphylococci (Fig. 1*B*), and it was predicted *in silico* to be extracellular. First, we confirmed its extracellular location by constructing PhoA-LacZ reporter fusions (44), whereby a fusion of the reporter chimera to the C-terminus of SosA conferred a phosphatase-positive, β-galatosidase-negative phenotype in *E. coli*, indicative of translocation across the membrane (*SI Appendix*, Fig. S5). Next, aiming at a functional characterization of its role in SosA activity, we constructed a series of C-terminally truncated variants by the successive elimination of ten amino acids (AAs) (Fig. 6*A*), resulting in four variants of SosA lacking between 10 and 40 of the C-terminal AAs. Strikingly, we observed that truncation of the 10 C-terminal AAs (and to some extent also removal of 20 C-terminal AAs) generated a hyper-potent inhibitor that gave rise to a severely compromised plating efficiency even at low inducer concentrations (Fig. 6*B*). Time-lapse microscopy revealed that cells producing

SosAd10 (SosA missing the last 10 AAs) had a dramatic phenotype, with prominent cell swelling and a reduction of the cell-cycle rate (Fig. 6*C* and Movie S3). The phenotypes from the plating assay correlated with the cell size measurements by flow cytometry (*SI Appendix*, Fig. S6), which indicated that cells expressing the 10 AA truncated protein were stalled in the non-dividing state that resulted in abnormal cell size, whereas those expressing full-length SosA were more transiently halted or delayed in cell division (*SI Appendix*, Fig. S6 and Movie S3). In contrast, deletion of 30 or 40 AAs from the C-terminal part eliminated the ability of SosA to inhibit cell division, as SosAd30 and SosAd40 gave comparable plating efficiency results to the control (Fig. 6*B*). This prompted us to investigate the relevance of the highly conserved residues located in the membrane-proximal part of the SosA C-terminal part by performing alanine substitutions within the protein. To this end, we used the hyper-active SosAd10 variant as a scaffold and found that while point mutations at AA positions 37 or 38 (E and Q) had no effect, point mutations at positions 40 or 41 (Y and E) partially inactivated and the mutations at positions 44 and 45 (D and H) completely abolished the cell-division inhibitory activity of the protein (*SI Appendix*, Fig. S7). Importantly, the inactive variants SosAd40 and SosAd10(44A) are presumably localized to the membrane, as are SosA and SosAd10, when evaluated by the PhoA-LacZ translocation assay (*SI Appendix*, Fig. S5). We conclude that conserved residues in the membrane-proximal segment of the extracellular C-terminal part of SosA are essential for inhibiting cell division, while truncation at the extreme C-terminus of the protein augments activity.

SosA is regulated by the CtpA protease. We reasoned that one explanation for the severe impact of the 10-AA-truncated SosA on cell division could be that the extreme C-terminus of SosA serves as an endogenous signal for proteolytic degradation, and its removal allowed the mutant to escape degradation and accumulate. We therefore searched the Nebraska Transposon Mutant

Library (45) for *S. aureus* protease mutants, specifically focusing on proteases considered to be membrane-localized. As a potential candidate, we identified a mutant in the carboxyl-terminal protease A (*ctpA*). The *S. aureus* CtpA protein is located at the cell-membrane/cell-wall fraction and is involved in stress tolerance and virulence in a mouse model of infection (46). Experiments involving the overproduction of the wildtype SosA protein in a *ctpA* mutant background (inactivated in *ctpA*) completely abolished cell viability, similarly to what was observed when the 10-AA-truncated SosA protein was overproduced in wildtype *S. aureus* cells (Fig. 7*A*). In agreement with this result, we found that the co-overproduction of SosA and CtpA in the *ctpA* mutant background alleviated the detrimental effect of SosA and that the degree of complementation depended on the relative expressional levels of the two proteins, such that at higher expression level of SosA only partial complementation was observed by concomitant CtpA expression (*SI Appendix*, Fig. S8). Furthermore, substantiating the negative regulatory role played by CtpA with respect to SosA, we noted that the *ctpA* mutant was moderately more sensitive to MMC (measured as a minimum inhibitory concentration) than wildtype *S. aureus*, but only when also encoding a functional *sosA* gene (Fig. 7*B*). Additionally, upon MMC-induced DNA damage, higher levels of the SosA protein accumulated in the *ctpA* mutant when compared to the wildtype (Fig. 7*C*). Altogether, based on these results, we propose that CtpA proteolytic activity acting on the extracellular C-terminus of SosA relieves SosA-mediated cell-division inhibition and allows growth to resume once DNA stress has ceased.

Discussion

Based on the results reported here, we propose the following model for regulation of cell division in the prolate spheroid bacterium *S. aureus* under DNA-damaging conditions (Fig. 8). During normal growth, the expression of *sosA* is repressed by the strong LexA repressor, but LexA is inactivated through autocleavage under SOS conditions, which results in the expression of *sosA*. It appears that the N-terminal autocleavage product of LexA needs to be further proteolytically processed for *sosA* expression to be fully induced (22), thus adding another layer of expressional control, suggesting tight regulation of the inhibitory protein. Upon derepression of LexA-regulated genes, SosA accumulates to levels that inhibit cell division without causing FtsZ delocalization nor preventing the assembly of downstream components, EzrA and GpsB, which are representatives of early and late cell division. The inhibitor appears to affect the progression and completion of septum formation via an interaction with PBP1. As a consequence of SosA activity, the cells appear synchronized at the stage of septum formation initiation, while an ongoing off-septal peptidoglycan synthesis leads to cell enlargement (*SI Appendix*, Fig. S3*C*). Once conditions are favorable for continued division, *sosA* expression is repressed, the membrane protease CtpA is involved in the removal or inactivation of SosA activity, and cell division resumes (Fig. 8).

The model illuminates several remaining unanswered questions. It will be particularly important to determine exactly how SosA affects the function of PBP1. In this context, it should be noted that our data fit well with the finding that the genetic depletion of PBP1 causes cell enlargement and incomplete septum formation (42). At present we cannot readily explain the peculiar finding that SosA and PBP1 seem to act in a synergistically lethal manner (Fig. 5*B*), though it is possible that the two proteins together constitute a signal to halt septum formation beyond a certain point.

Alternatively, the synergistic effects could depend on stoichiometry and physical accessibility in the sense that PBP1 might engage in a non-productive complex with SosA, more efficiently preventing residual and functional PBP1 access to the site. We keep in mind that SosA may also interact with PBP3 and DivIC (Fig. 5*A*), and these relationships should also be investigated. Interactions between the *S. aureus* divisome components constitute a complex web, and in the bacterial two-hybrid study, PBP1 interacted with DivIC, which in turn interacted with PBP3 (38). Thus, the inhibitory activity of SosA could be multifactorial.

An analysis of the AA sequence of SosA indicated that the N-terminal part contained a TM domain while the C-terminal was located extracellularly. The hypothesis that the TM domain promotes localization to the cellular membrane was supported by PhoA-LacZ fusion to SosA and by various point and deletion mutants of the fusion protein (*SI Appendix*, Fig. S5). The abrogation of activity by the 40-AA-truncation as well as by a single alanine substitution (D44A) suggests that this segment is essential for correct localization to the septum or, perhaps more interestingly, that the actual motif for cell-division inhibition is localized at the exterior of the membrane. If PBP1 interference indeed lies within this segment of SosA, it could provide a novel paradigm for interference with penicillin-binding proteins that could supplement the transpeptidase-inhibitory activity exerted by β-lactam antibiotics.

Endogenous cell-division inhibition must be stringently regulated, as demonstrated by pioneering work showing that SulA of *E. coli* is degraded by the Lon protease (15). Similarly, YneA from *B. subtilis* was reported to be regulated by proteolysis (36), while in *B. megaterium*, the temporal expression of a YneA homologue has been suggested to be due to mRNA instability (25). We demonstrated that a minor truncation of the C-terminus of SosA yields a hyper-potent cell-division

inhibitor (Fig. 6), which led us to speculate that the extreme C-terminus serves as a signal for proteolysis. We identified a CtpA protease-deficient strain in which SosA appeared to accumulate and had an increased detrimental effect compared to the wildtype background. Bacterial carboxy-terminal proteases are poorly characterized, particularly with respect to their substrate preferences. Due to this protein's involvement in stress tolerance and virulence in *S. aureus* (46) and its predicted carboxy-terminal activity, we tested its effect in conjunction with SosA and propose that CtpA specifically regulates SOS-induced cell-division inhibition in staphylococci, likely via recognition of the C-terminus of SosA. Biochemical evidence for such a direct activity will be needed, and at present we cannot exclude an indirect effect. Interestingly, a point mutation in *B. subtilis* YneA at its extreme C-terminus generated a stabilized yet functional variant of the cell-division inhibitor (36), suggesting that YneA and SosA may be degraded by similar mechanisms. Of note, carboxy-terminal proteases are ubiquitous in bacterial genera, and homologs of CtpA are found in other gram-positive species, such as *B. subtilis* and *L. monocytogenes.* Hence, the CtpA-like proteases could represent functional homologs of the *E. coli* Lon protease, allowing negative regulation of endogenous cell-division inhibition more broadly amongst gram-positives.

SosA may also prove to be a useful tool for scientists conducting studies into bacterial cell division, which have recently benefitted from the development of genetic tools and highly sophisticated microscopic imaging technologies. However, most often bacteria grow as an unsynchronized population with individual cells in different phases of cell division, making it challenging to order the temporal events that occur during cell-cycle progression, DNA replication, and division. Essentially, SosA is involved in halting the *S. aureus* cell cycle at a specific morphological stage, e.g. following the piecrust formation, and we anticipate that the exploitation of this function may

constitute a useful tool for the generation of synchronized staphylococcal cells for experimental purposes.

Apart from its basic biological interest, the bacterial cell-division process may constitute an unexhausted source of novel therapeutic targets (1,2). We believe that SosA could be a natural scaffold, and the study of this protein can provide new therapeutically accessible targets that would interfere with an essential process in *S. aureus* and other staphylococci.

Materials and Methods

Bacterial strains and plasmids used in this work. The bacterial strains and plasmids used in this study are listed in *SI Appendix*, Table S1 and Table S2, respectively. *E. coli* strains were grown in Luria-Bertani medium (Oxoid) or on LB agar (Oxoid). *S. aureus* strains were grown in Tryptic Soy Broth (TSB) or on Tryptic Soy Agar (TSA) (both Oxoid). Ampicillin (100 µg/ml), chloramphenicol (10 µg/ml), or erythromycin (5 µg/ml) were added when appropriate. Anhydrotetracycline (AHT) (Sigma-Aldrich) and Isopropyl β-D-1-thiogalactopyranoside (IPTG) (Thermo Scientific) were used as inducers for protein expression.

Construction of strains and plasmids. All oligonucleotides used are listed in *SI Appendix*, Table S3. *S. aureus* 8325-4Δ*sosA* is a clean deletion of *sosA* (SAOUHSC_01334) in strain 8325-4 obtained by allelic replacement using the temperature-sensitive shuttle vector pIMAY (47). 1 kb regions up- and downstream of *sosA* were PCR amplified (Phusion Hot Start II DNA Polymerase, Thermo Scientific) using primer pairs Up-sosA_fw-KpnI/Up-sosA_rev and Dw-sosA_fw/Dw-sosA_rev-SacI, respectively, and subsequently joined in a spliced overhang PCR using Up-sosA_fw-KpnI/Dw-

sosA_rev-SacI. The resulting deletion fragment was cloned into pIMAY via KpnI/SacI, generating pIMAY-Δ*sosA*, purified from *E. coli* DC10B and transformed into *S. aureus* subsequently maintained at 28°C. Chromosomal integration of the plasmid was performed at 37°C under selective conditions (chloramphenicol) followed by passage at 28°C without antibiotic selection and final plating on TSA containing 500 ng/ml of AHT for plasmid counterselection. Colonies were replica-plated to select for sensitivity towards chloramphenicol and successful allelic exchange were screened for by PCR amplification using primer pairs Ctrl_dsosA_F/Ctrl_dsosA_R positioned outside *sosA* and Fwd_MCS/Rev_MCS targeting the vector, respectively. The allelic replacement procedure was identical for *S. aureus* JE2 to create JE2Δ*sosA*.

The chromosomal transposon insertion mutation in *ctpA* conferring erythromycin resistance was obtained from the Nebraska Transposon Mutant Library (NTML, NE847) (45) and was moved by transduction (phage Φ11) to *S. aureus* JE2, JE2Δ*sosA*, S. *aureus* 8325-4 and 8325-4Δ*sosA*, resulting in JE2-*ctpA*, JE2Δ*sosA*-*ctpA*, 8325-4-*ctpA* and 8325-4Δ*sosA*-*ctpA*, respectively. JE2-*ctpA*(−erm), an erythromycin-sensitive derivative, was generated by elimination of the transposon-encoded *ermB* in JE2-*ctpA* by allelic exchange using the pTnT vector using temperature-mediated chromosomal integration and *secY*-mediated counterselection as described before (48).

All plasmid constructs mentioned below were cloned in E. coli IM08B (49) from where they were transformed into *S. aureus* strains. For complementation of the *sosA* knockout, the *sosA* gene with its native promoter was PCR amplified from strain 8325-4 using primers Up-sosA-promo_SalI and Dw-sosA_EcoRI and cloned into designated restriction sites in plasmid pJC1112 (50). The resulting plasmid (pJC1112-*sosA*) was transformed into the integration-proficient strain RN9011, creating RN9011-*sosA*-compl. when selected with erythromycin. The chromosomally integrated plasmid

was transduced into 8325-4Δ*sosA*, resulting in 8325-4Δ*sosA*-compl. For *sosA* expression the *sosA* gene including its predicted ribosomal binding site was cloned into the BglII and EcoRI sites of pRAB12-*lacZ* (51) using primers Up-sosA_BglII/Dw-sosA_EcoRI, at the same time eliminating the *lacZ* reporter gene. The resulting plasmid was called pSosA. Generation of plasmids encoding C-terminally truncated variants of SosA was obtained by PCR amplification of DNA fragments using Up-sosA_BglII and downstream primers Dw-sosA(d10)_EcoRI to Dw-sosA(d40)_EcoRI, all equipped with premature stop codons. The PCR products were ligated into pRAB12-*lacZ* using BglII and EcoRI cut sites to create pSosAd10, pSosAd20, pSosAd30 and pSosAd40. Single and double amino acid substitutions (alanine) in the SosAd10 protein were obtained by cloning commercially synthesized DNA fragments (Twist Bioscience) into pRAB12-*lacZ* using the same restriction sites. Plasmids for *pbpA* or *ctpA* expression, pPBP1 and pCtpA, were constructed by cloning the *pbpA* and *ctpA* genes behind the P_{spac} promoter in pSK9067 (52) using primer pairs pbpA_F-SalI/pbpA_R-EcoRI and ctpA_F-SalI/ctpA_R-EcoRI, respectively. A plasmid for *pbpA** expression was constructed by use of the same primer pair but using pMAD-PBP1* (53) as a template. For membrane topology analysis using pKTop (44), *sosA*, *sosAd10*, *sosAd10(44A)* and *sosAd40* were PCR amplified from respective expression constructs using primer SosA_F-BamHI and primers SosA_R-KpnI, SosAd10_R-KpnI or SosAd40_R-KpnI, respectively, and cloned in frame in front of the *phoA*-*lacZ* chimeric gene using BamHI/KpnI restriction sites.

In order to construct JE2 strains producing a fluorescent fusion of FtsZ, EzrA or GpsB in the presence of the *sosA* expression plasmid, JE2 pSosA was transduced with a lysate from SH4665 (SH1000 pCQ11-FtsZ-eYFP), JGL227 (SH1000 *ezrA*-*gfp*+) or JGL228 (SH1000 *gpsB*-*gfp*+), resulting in SJF4694 (JE2 pRAB12-*lacZ* pCQ11-FtsZ-eYFP), SJF4696 (JE2 pRAB12-*lacZ ezrA*-*gfp*+) and SJF4699 (JE2 pRAB12-*lacZ gpsB -gfp*+), respectively. Control strains SJF4693 (JE2 pRAB12-*lacZ* pCQ11-FtsZ-

eYFP), SJF4696 (JE2 pRAB12-*lacZ ezrA-gfp*+) and SJF4699 (JE2 pRAB12-*lacZ gpsB-gfp*+) were constructed by a phage transduction of JE2 pRAB12-*lacZ* with lysates from SH4665 (SH1000 pCQ11-FtsZ-eYFP), JGL227 (SH1000 *ezrA-gfp*+) or JGL228 (SH1000 *gpsB-gfp*+), respectively. To induce FtsZ-eYFP production in SJF4693 and SJF4694, cells were grown in the presence of 50 µM IPTG.

In order to screen for interaction of SosA with cell-division/cell wall synthesis proteins of *S. aureus*, *sosA* was amplified from *S. aureus* SH1000 genomic DNA using primers ALB133 and ALB134, and ligated into pUT18C using BamHI/EcoRI cut sites, resulting in pT18-SosA. All fusion constructs to T25 and control vectors were generated previously (38, 54-56, *SI Appendix*, Table S2).

Determination of OD_{600} and CFU after MMC treatment. Strains were grown overnight on TSA plates and used for inoculating TSB and allowed to grow to OD_{600} = 0.05 when Mitomycin C (MMC from *Streptomyces caespitosus*, Sigma-Aldrich) was added. Cell density was monitored by OD_{600} measurements at intervals onwards and samples were withdrawn to determine culture colony forming units by serial dilution in 0.9% w/v NaCl and plating on TSA.

Flow cytometry. Cell size distributions of cultures were arbitrarily quantified by flow cytometry using the forward scatter signal (FSC-A) acquired on a BD Accuri™ C6 flow cytometer (BD Biosciences). Cell samples were diluted in 0.9% w/v NaCl to an approximate density of 10^6 cells/ml and sonicated briefly to allow acquisition of scatter signal from single cells predominantly. Sonication was performed with a Bandelin sonopuls HD2070/UW2070 apparatus (Bandelin electronics, Germany) fitted with the MS 73 probe. Ten pulses of 500 msec were given at 50% power. All flow cytometry experiments were independently repeated at least twice with similar results.

Plating assays. Spot dilution was used to evaluate plating efficiency of strains carrying various plasmid constructs. Strains were grown exponentially until an approximate OD_{600} of 0.5 under plasmid selective conditions. Strains were then ten-fold serially diluted in 0.9% w/v NaCl and positioned as 10 µl spots on TSA containing selective antibiotics with/without inducer at indicated concentrations and incubated at 37°C overnight. All spot plating assays were independently repeated with similar results.

Labelling *S. aureus* with HADA

Cells grown to mid-exponential phase (OD_{600} ~ 0.5) were incubated with 500 µM HADA at 37°C for 5 min. Cells were then washed by centrifugation and resuspension in PBS.

Labelling *S. aureus* with NHS ester

Labelling with NHS ester was performed as described before (33). Briefly, cells grown to mid-exponential phase (OD_{600} ~0.5) were collected by centrifugation and growth medium was discarded. Cells were resuspended in PBS containing 8 µg ml^{-1} Alexa Fluor 647 NHS ester (Invitrogen) and incubated at room temperature for 5 min. Cells were washed by centrifugation and resuspension in PBS.

Fixing

Cells were fixed by incubation in 4% (w/v) paraformaldehyde at room temperature for 30 min.

Widefield Epifluorescence Microscopy

Fixed cells were dried onto a poly-L-Lysine coated slide and mounted in PBS. Imaging was performed using either a Nikon Ti Inverted microscope fitted with a Lumencor Spectra X light engine or a v4 DeltaVision OMX 3D-SIM system (Applied Precision, GE Healthcare, Issaquah, USA).

3D Structured Illumination Microscopy

A high precision cover slip (High-precision, No.1.5H, 22x22mm, 170±5 µm, Marienfeld) was cleaned by sonicating in 1 M KOH for 15 min at room temperature. The coverslip was washed with water and incubated in 0.01% (w/v) poly-L-lysine solution (Sigma) for 30 min at room temperature. The coverslip was rinsed with water and dried with nitrogen. Fixed cells were dried onto the poly-L-Lysine coated cover slip and mounted on a slide with SlowFade Diamond (Invitrogen). 3D SIM visualisation was performed using a v4 DeltaVision OMX 3D-SIM system (Applied Precision, GE Healthcare, Issaquah, USA) equipped with a Plan Apo 60x, 1.42 NA oil objective, using 1.514 immersion oil, a 642 nm laser and a standard excitation/emission filter set (683/40). For each z-section, a sample was imaged in 5 phase shifts and 3 angles. The z-sections were 0.125 nm in depth. Raw data were reconstructed with the Softworx software (GE Healthcare) using OTFs optimized for the specific wavelength and oil used.

Time-lapse microscopy. Strains were grown overnight in TSB medium at 37°C, then diluted 100 times in fresh TSB and grown until OD = 0.1. Cells were washed once with fresh TSB and spotted onto TSB-acrylamide (10%) pads previously incubated for 2h in TSB medium supplemented, when appropriate, with 0.04 µg/mL mitomycin C (MMC) or 200 ng/mL anhydrotetracycline (AHT). Pads were placed into a Gene frame (Thermo Fisher Scientific) and sealed with a cover glass. Phase-contrast images were acquired on a DV Elite microscope (GE healthcare) equipped with a sCMOS (PCO) camera and a 100x oil-immersion objective. Images were acquired with 200 ms exposure time every 4 minutes for at least 6 h at 37°C using Softworx (Applied Precision) software. Images were analyzed using Fiji (http://fiji.sc).

Western blot analysis. A custom peptide (EZBiolab) comprising AAs 35-77 of SosA was conjugated, through NH_2 (N-terminus) and NH_2 of lysines (K) to a KLH carrier protein using glutaraldehyde and used for antibody production in rabbits (Covalab). Bacterial cells were pelleted and frozen immediately at -80°C before being lysed in TE-buffer by bead-beating (Fastprep-24™, MP Biomedicals). The protein concentration of the lysates was measured using the Qubit™ Protein Assay Kit (ThermoFisher Scientific) and were normalized to equal amounts of protein, separated on NuPAGE® 4-12% Bis-Tris gels using MES buffer and the XCell sure-lock mini-cell system (ThermoFisher Scientific), transferred to a polyvinylidene difluoride membrane(PVDF) and probed with primary antibody diluted 1:500. Bound antibody was detected with the WesternBreeze® Chemiluminescent Kit, anti-rabbit according to the instructions from the manufacturer (ThermoFisher Scientific).

Bacterial two-hybrid assay. Interactions between SosA and proteins involved in cell division and cell wall synthesis of *S. aureus* were tested using *E.coli* BTH101 (Δ*cyaA*) cotransformed with pT18-SosA and a plasmid carrying a fusion of T25 with a cell-division or cell wall synthesis protein on minimal medium as previously described (38).

Acknowledgements

This work was supported by grants from the Danish Council for Independent Research – Technology and Production (1337-00129 and 1335-00772) to M.S.B., by the Danish National Research Foundation (DNRF120) to H.I., and by the Medical Research Council (MR/K015753/1 to the Wolfson Light Microscopy Facility at the University of Sheffield and MR/N002679/1). We would like to thank Prof Simon Jones (University of Sheffield) for the HADA dye.

M.S.B., K.W., P.K., M.T.C., S.J.F., and H.I. conceived and designed the study. Experiments were performed by M.S.B., K.W., C.G., and A.L.B. M.S.B. K.W., C.G., G.L., D.F., J.-W.V., S.J.F., and H.I. contributed to analysis of data and drafting of the manuscript. All authors read and approved the final manuscript.

References

1. Sass P, Brötz-Oesterhelt H. 2013. Bacterial cell division as a target for new antibiotics. Curr Opin Microbiol 16:522-530.
2. Lock RL, Harry EJ. 2008. Cell-division inhibitors: new insights for future antibiotics. Nat Rev Drug Discov 7:324-338.
3. Robinson A, Causer RJ, Dixon NE. 2012. Architecture and conservation of the bacterial DNA replication machinery, an underexploited drug target. Curr Drug Targets 13:352-372.
4. Adams DW, Errington J. 2009. Bacterial cell division: assembly, maintenance and disassembly of the Z ring. Nat Rev Microbiol 7:642-653.
5. Baharoglu Z, Mazel D. 2014. SOS, the formidable strategy of bacteria against aggressions. FEMS Microbiol Rev 38:1126-1145.
6. Kreuzer KN. 2013. DNA damage responses in prokaryotes: regulating gene expression, modulating growth patterns, and manipulating replication forks. Cold Spring Harb Perspect Biol 5:a012674.
7. Kelley WL. 2006. Lex marks the spot: the virulent side of SOS and a closer look at the LexA regulon. Mol Microbiol 62:1228-1238.

8. Huisman O, D'Ari R. 1981. An inducible DNA replication-cell division coupling mechanism in E. coli. Nature 290:797-799.
9. Huisman O, D'Ari R, Gottesman S. 1984. Cell-division control in Escherichia coli: specific induction of the SOS function SfiA protein is sufficient to block septation. Proc Natl Acad Sci U S A 81:4490-4494.
10. Jones C, Holland IB. 1985. Role of the SulB (FtsZ) protein in division inhibition during the SOS response in Escherichia coli: FtsZ stabilizes the inhibitor SulA in maxicells. Proc Natl Acad Sci U S A 82:6045-6049.
11. Higashitani A, Higashitani N, Horiuchi K. 1995. A cell division inhibitor SulA of Escherichia coli directly interacts with FtsZ through GTP hydrolysis. Biochem Biophys Res Commun 209:198-204.
12. Mukherjee A, Cao C, Lutkenhaus J. 1998. Inhibition of FtsZ polymerization by SulA, an inhibitor of septation in Escherichia coli. Proc Natl Acad Sci U S A 95:2885-2890.
13. Cordell SC, Robinson E J, Lowe J. 2003. Crystal structure of the SOS cell division inhibitor SulA and in complex with FtsZ. Proc Natl Acad Sci U S A 100:7889-7894.
14. Schoemaker JM, Gayda RC, Markovitz A. 1984. Regulation of cell division in Escherichia coli: SOS induction and cellular location of the sulA protein, a key to lon-associated filamentation and death. J Bacteriol 158:551-561.
15. Mizusawa S, Gottesman S. 1983. Protein degradation in Escherichia coli: the lon gene controls the stability of sulA protein. Proc Natl Acad Sci U S A 80:358-362.
16. Modell JW, Hopkins AC, Laub MT. 2011. A DNA damage checkpoint in Caulobacter crescentus inhibits cell division through a direct interaction with FtsW. Genes Dev 25:1328-1343.

17. Tzagoloff H, Novick R. 1977. Geometry of cell division in Staphylococcus aureus. J Bacteriol 129:343-350.

18. Turner RD, Ratcliffe EC, Wheeler R, Golestanian R, Hobbs JK, Foster SJ. 2010. Peptidoglycan architecture can specify division planes in Staphylococcus aureus. Nat Commun 1:26.

19. Pinho MG, Kjos M, Veening JW. 2013. How to get (a)round: mechanisms controlling growth and division of coccoid bacteria. Nat Rev Microbiol 11:601-614.

20. Cirz RT, Jones MB, Gingles NA, Minogue TD, Jarrahi B, Peterson SN, Romesberg FE. 2007. Complete and SOS-mediated response of Staphylococcus aureus to the antibiotic ciprofloxacin. J Bacteriol 189:531-539.

21. Anderson KL, Roberts C, Disz T, Vonstein V, Hwang K, Overbeek R, Olson PD, Projan SJ, Dunman PM. 2006. Characterization of the Staphylococcus aureus heat shock, cold shock, stringent, and SOS responses and their effects on log-phase mRNA turnover. J Bacteriol 188:6739-6756.

22. Cohn MT, Kjelgaard P, Frees D, Penadés JR, Ingmer H. 2011. Clp-dependent proteolysis of the LexA N-terminal domain in Staphylococcus aureus. Microbiology 157:677-684.

23. Mesak LR, Miao V, Davies J. 2008. Effects of subinhibitory concentrations of antibiotics on SOS and DNA repair gene expression in Staphylococcus aureus. Antimicrob Agents Chemother 52:3394-3397.

24. Kawai Y, Moriya S, Ogasawara N. 2003. Identification of a protein, YneA, responsible for cell division suppression during the SOS response in Bacillus subtilis. Mol Microbiol 47: 1113-1122.

25. Buchholz M, Nahrstedt H, Pillukat MH, Deppe V, Meinhardt F. 2013. yneA mRNA instability is involved in temporary inhibition of cell division during the SOS response of Bacillus megaterium. Microbiology 159:1564-1574.
26. van der Veen S, Hain T, Wouters JA, Hossain H, de Vos WM, Abee T, Chakraborty T Wells-Bennik MH. 2007. The heat-shock response of Listeria monocytogenes comprises genes involved in heat shock, cell division, cell wall synthesis, and the SOS response. Microbiology 153:3593-3607.
27. van der Veen S, van Schalkwijk S, Molenaar D, de Vos WM, Abee T, Wells-Bennik MH. 2010. The SOS response of Listeria monocytogenes is involved in stress resistance and mutagenesis. Microbiology 156:374-384.
28. Chauhan A, Lofton H, Maloney E, Moore J, Fol M, Madiraju MV, Rajagopalan M. 2006. Interference of Mycobacterium tuberculosis cell division by Rv2719c, a cell wall hydrolase. Mol Microbiol 62:132-147.
29. Ogino H, Teramoto H, Inui M, Yukawa H. 2008. DivS, a novel SOS-inducible cell-division suppressor in Corynebacterium glutamicum. Mol Microbiol 67:597-608.
30. Buist G, Steen A, Kok J, Kuipers OP. 2008. LysM, a widely distributed protein motif for binding to (peptido)glycans. Mol Microbiol 68:838-847.
31. Mesnage S, Dellarole M, Baxter NJ, Rouget JB, Dimitrov JD, Wang N, Fujimoto Y, Hounslow AM, Lacroix-Desmazes S, Fukase K, Foster SJ, Williamson MP. 2014. Molecular basis for bacterial peptidoglycan recognition by LysM domains. Nat Commun 5:4269.
32. Monteiro JM, Fernandes PB, Vaz F, Pereira AR, Tavares AC, Ferreira MT, Pereira PM, Veiga H, Kuru E, VanNieuwenhze MS, Brun YV, Filipe SR, Pinho MG. 2015. Cell shape dynamics during the staphylococcal cell cycle. Nat Commun 6:8055.

33. Lund VA, Wacnik K, Turner RD, Cotterell BE, Walther CG, Fenn SJ, Grein F, Wollman AJ, Leake MC, Olivier N, Cadby A, Mesnage S, Jones S, Foster SJ. 2018. Molecular coordination of Staphylococcus aureus cell division. Elife 7:e32057.
34. Monteiro JM, Pereira AR, Reichmann NT, Saraiva BM, Fernandes PB, Veiga H, Tavares AC, Santos M, Ferreira MT, Macário V, VanNieuwenhze MS, Filipe SR, Pinho MG. 2018. Peptidoglycan synthesis drives an FtsZ-treadmilling-independent step of cytokinesis. Nature 554:528-532.
35. Vadrevu IS, Lofton H, Sarva K, Blasczyk E, Plocinska R, Chinnaswamy J, Madiraju M, Rajagopalan M. 2011. ChiZ levels modulate cell division process in mycobacteria. Tuberculosis (Edinb) 91:S128-135.
36. Mo AH, Burkholder WF. 2010. YneA, an SOS-induced inhibitor of cell division in Bacillus subtilis, is regulated posttranslationally and requires the transmembrane region for activity. J Bacteriol 192:3159-3173.
37. Tsirigos KD, Peters C, Shu N, Käll L, Elofsson A. 2015. The TOPCONS web server for consensus prediction of membrane protein topology and signal peptides. Nucleic Acids Res 43:W401-7.
38. Steele VR, Bottomley AL, Garcia-Lara J, Kasturiarachchi J, Foster SJ. 2011. Multiple essential roles for EzrA in cell division of Staphylococcus aureus. Mol Microbiol 80:542-555.
39. Bottomley AL, Kabli AF, Hurd AF, Turner RD, Garcia-Lara J, Foster SJ. 2014. Staphylococcus aureus DivIB is a peptidoglycan-binding protein that is required for a morphological checkpoint in cell division. Mol Microbiol 94:1041-1064.
40. Gamba P, Veening JW, Saunders NJ, Hamoen LW, Daniel RA. 2009. Two-step assembly dynamics of the Bacillus subtilis divisome. J Bacteriol 191:4186-4194.

41. Kawai Y, Ogasawara N. 2006. Bacillus subtilis EzrA and FtsL synergistically regulate FtsZ ring dynamics during cell division. Microbiology 152:1129-1141.

42. Pereira SF, Henriques AO, Pinho MG, de Lencastre H, Tomasz A. 2007. Role of PBP1 in cell division of Staphylococcus aureus. J Bacteriol 189:3525-3531.

43. Pereira SF, Henriques AO, Pinho MG, de Lencastre H, Tomasz A. 2009. Evidence for a dual role of PBP1 in the cell division and cell separation of Staphylococcus aureus. Mol Microbiol 72:895-904.

44. Karimova G, Ladant D. 2017. Defining Membrane Protein Topology Using pho-lac Reporter Fusions. Methods Mol Biol 1615:129-142.

45. Fey PD, Endres JL, Yajjala VK, Widhelm TJ, Boissy RJ, Bose JL, Bayles KW. 2013. A genetic resource for rapid and comprehensive phenotype screening of nonessential Staphylococcus aureus genes. MBio 4:e00537-12.

46. Carroll RK, Rivera FE, Cavaco CK, Johnson GM, Martin D, Shaw LN. 2014. The lone S41 family C-terminal processing protease in Staphylococcus aureus is localized to the cell wall and contributes to virulence. Microbiology 160:1737-1748.

47. Monk IR, Shah IM, Xu M, Tan MW, Foster TJ. 2012. Transforming the untransformable: application of direct transformation to manipulate genetically Staphylococcus aureus and Staphylococcus epidermidis. MBio 3:e00277-11.

48. Bose JL, Fey PD, Bayles KW. 2013. Genetic tools to enhance the study of gene function and regulation in Staphylococcus aureus. Appl Environ Microbiol 79:2218-2224.

49. Monk IR, Tree JJ, Howden BP, Stinear TP, Foster TJ. 2015. Complete Bypass of Restriction Systems for Major Staphylococcus aureus Lineages. MBio 6:e00308-15.

50. Chen J, Yoong P, Ram G, Torres VJ, Novick RP. 2014. Single-copy vectors for integration at the SaPI1 attachment site for Staphylococcus aureus. Plasmid 76:1-7.

51. Helle L, Kull M, Mayer S, Marincola G, Zelder ME, Goerke C, Wolz C, Bertram R. 2011. Vectors for improved Tet repressor-dependent gradual gene induction or silencing in Staphylococcus aureus. Microbiology 157:3314-3323.

52. Brzoska AJ, Firth N. 2013. Two-plasmid vector system for independently controlled expression of green and red fluorescent fusion proteins in Staphylococcus aureus. Appl Environ Microbiol 79:3133-3136.

53. Wacnik K. 2016. Dissecting cell division in the human pathogen Staphylococcus aureus. PhD Thesis. University of Sheffield.

54. Karimova G, Pidoux J, Ullmann A, Ladant D. 1998. A bacterial two-hybrid system based on a reconstituted signal transduction pathway. Proc Natl Acad Sci U S A 95:5752-5756.

55. Claessen D, Emmins R, Hamoen LW, Daniel RA, Errington J, Edwards DH. 2008. Control of the cell elongation-division cycle by shuttling of PBP1 protein in Bacillus subtilis. Mol Microbiol 68:1029-1046.

56. Bottomley AL, Liew ATF, Kusuma KD, Peterson E, Seidel L, Foster SJ, Harry EJ. 2017. Coordination of Chromosome Segregation and Cell Division in Staphylococcus aureus. Front Microbiol 8:1575.

Figures

Figure 1

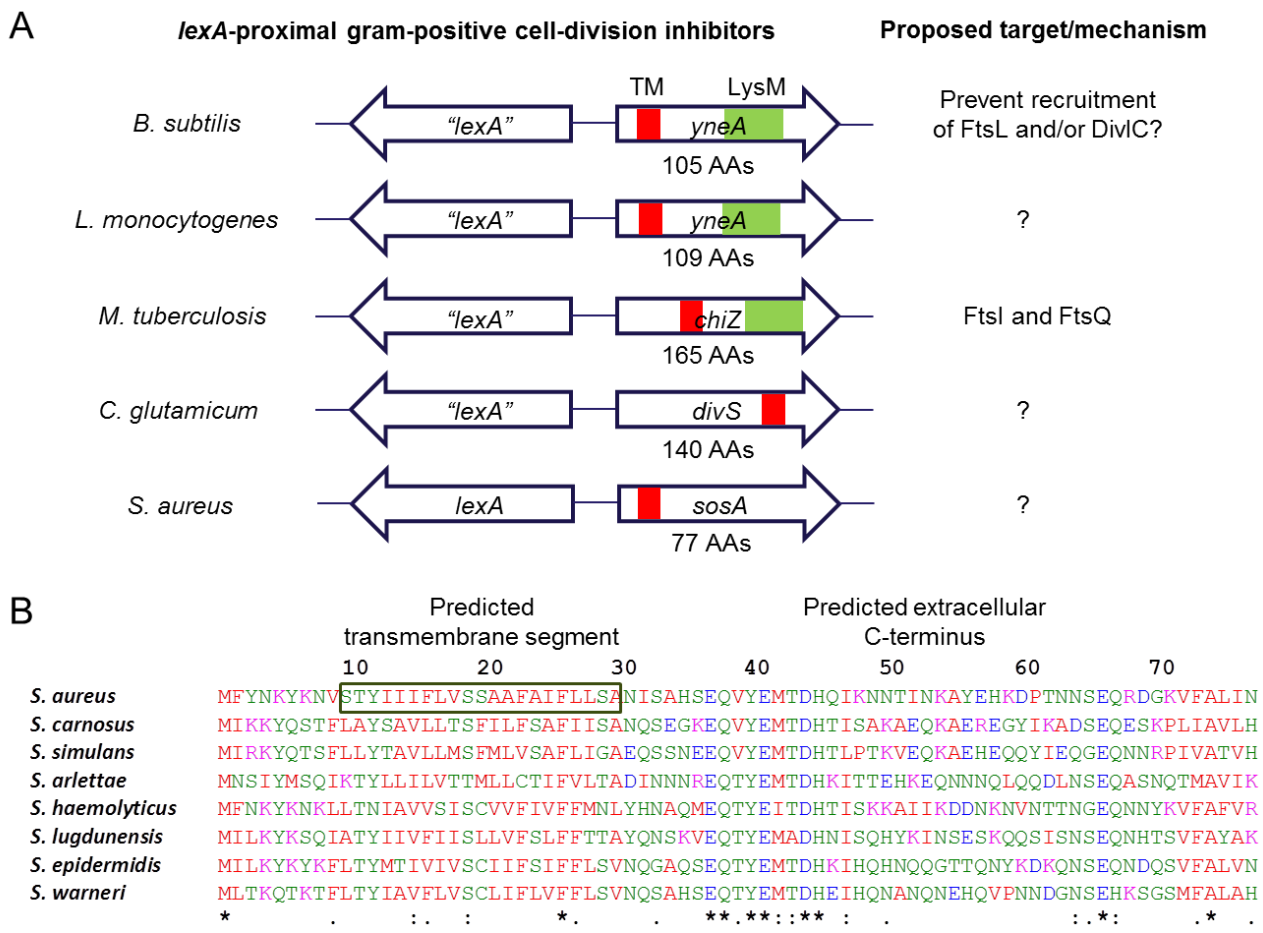

Fig 1 Gram-positive SOS-controlled cell-division inhibitors. (*A*) Schematic representation of genes encoding characterized gram-positive SOS-regulated cell-division inhibitors (not drawn to scale) including the uncharacterized *sosA* from *S. aureus*. Despite considerable sequence divergence, these genes are commonly chromosomally co-localized with *lexA* homologous genes. The cell-division inhibitors carry a single transmembrane domain (TM), and several proteins have an additional LysM domain. (*B*) Alignment (CLUSTAL O[1.2.4]) of SosA sequences deduced from open reading frames next to *lexA* in *S. aureus* strain 8325-4 (YP_499864) and seven *Staphylococcus* species: *S. carnosus* (CAL27889), *S. simulans* (AMG96201), *S. arlettae* (EJY94737), *S. haemolyticus*

(YP_253482), *S. lugdunensis* (YP_003471776), *S. epidermidis* (YP_188489), and *S. warneri* (EEQ79882). The proteins are 77 amino acids long and are characterized by a predicted transmembrane segment at AAs 10-30 (for *S. aureus* SosA) and a predicted extracellular C-terminal (TOPCONS [37]) with considerable sequence conservation at the membrane-proximal portion ("*" indicates fully conserved residues, ":" indicates conservation of residues with highly similar properties).

Figure 2

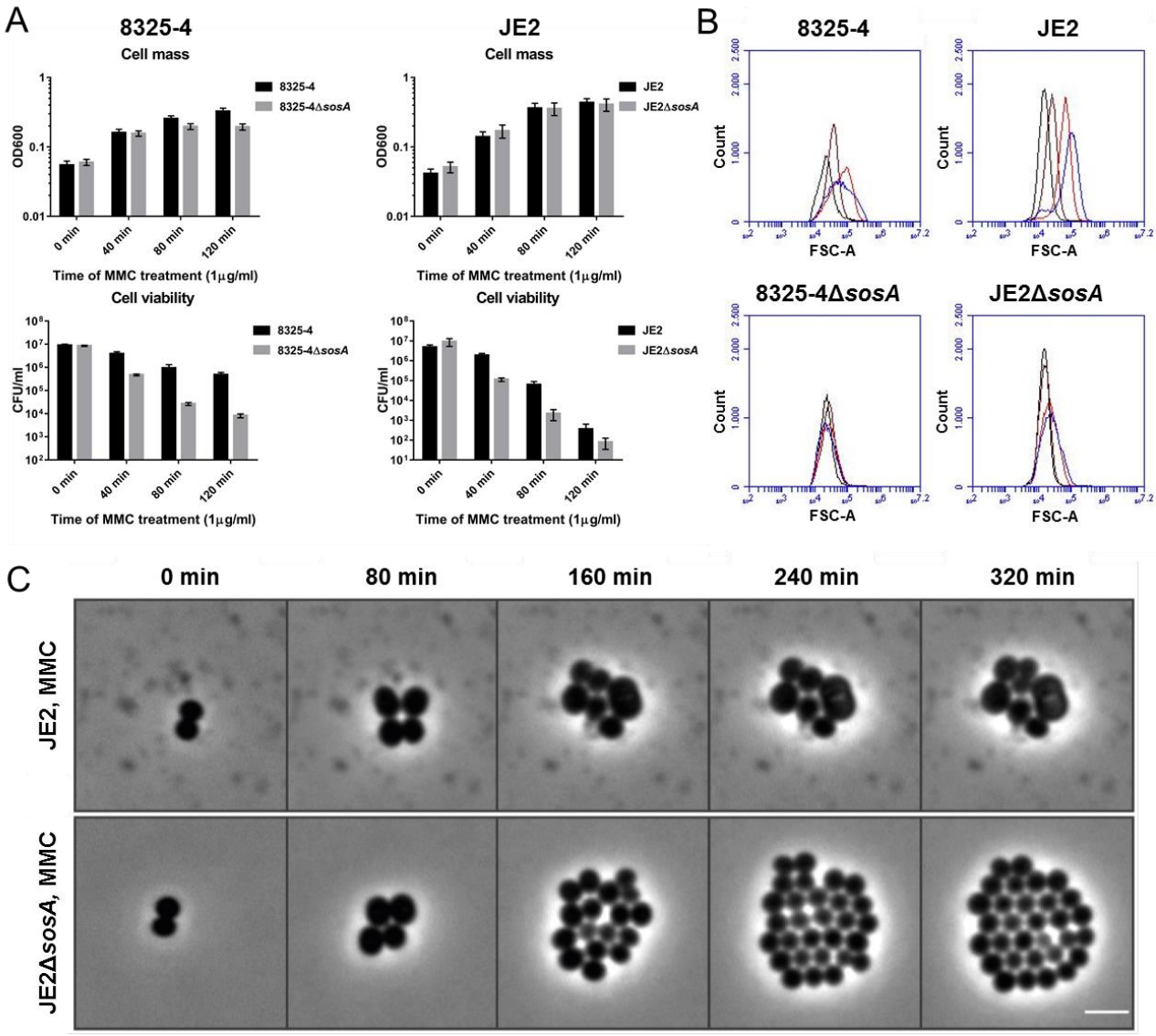

Fig 2 The *sosA* gene supports the survival of *S. aureus* subjected to lethal DNA damage and is involved in bacterial swelling. (*A*) Culture optical density at 600 nm and cell viability of *S. aureus* strains 8325-4 and JE2 in comparison with their respective *ΔsosA* mutants upon challenge with a lethal dose of mitomycin C (MMC, 1 µg/ml) for two hours. Error bars represent the standard deviation from three biological replicates. (*B*) Cell size of 8325-4 and JE2 wildtype and *ΔsosA* mutants during the mitomycin C killing experiment estimated arbitrarily by flow cytometry (FSC-A). Cells were grown exponentially prior to MMC addition at an OD_{600} of 0.05. Samples were taken after 0 (black), 40 (brown), 80 (red), and 120 (blue) minutes of incubation with MMC. (*C*) Effect of MMC treatment (0.04 µg/mL) on cell shape and cell number of JE2 wildtype and JE2Δ*sosA* as visualized by time-lapse phase-contrast microscopy. Scale bar represents 2 µm.

Figure 3

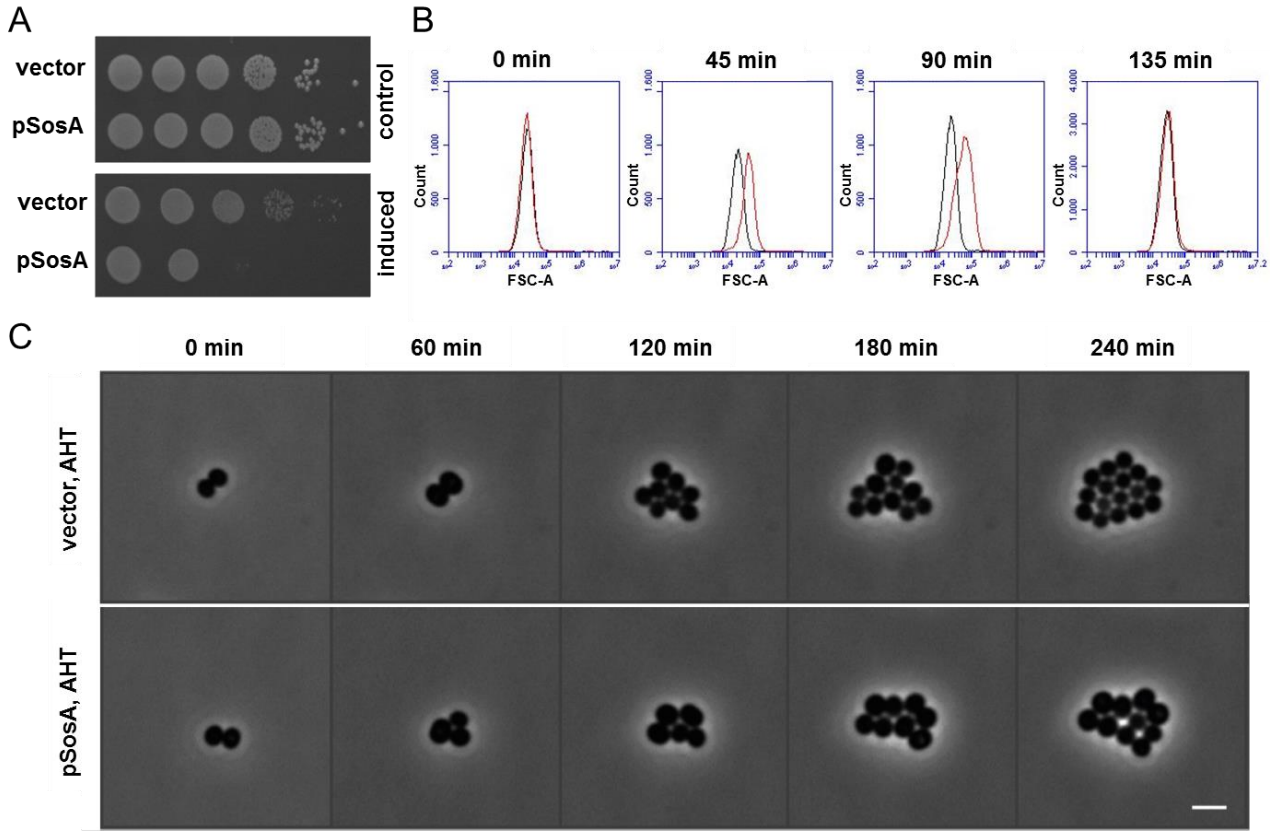

Fig 3 Expression of *sosA* alone interferes with *S. aureus* growth. (*A*) The effect of a controlled expression of *sosA* on the ability to form colonies was assessed in *S. aureus* RN4220. Strains carrying either the vector control (vector) or *sosA* under an anhydrotetracycline (AHT)-inducible promoter (pSosA) were grown exponentially to an OD_{600} of 0.5, serially 10-fold diluted, and plated on TSA plates in the presence (induced) or absence (control) of TSA+300 ng/ml of AHT. The plates were incubated overnight at 37°C and imaged. (*B*) Evaluation of cell size distribution by flow cytometry (FSC-A) of *S. aureus* RN4220 containing the control vector (black) or pSosA (red). Cells were grown exponentially prior to induction with 100 ng/ml of AHT. At the indicated time points, the cells were collected and analyzed by flow cytometry. (*C*) Visualization of cell size increase and

reduction of cell number of JE2/pRAB12-*lacZ* (control) and JE2/pRAB12-*sosA* in the presence of 200 ng/mL of AHT by time-lapse phase-contrast microscopy at 37°C. Scale bar represents 2 µm.

Figure 4

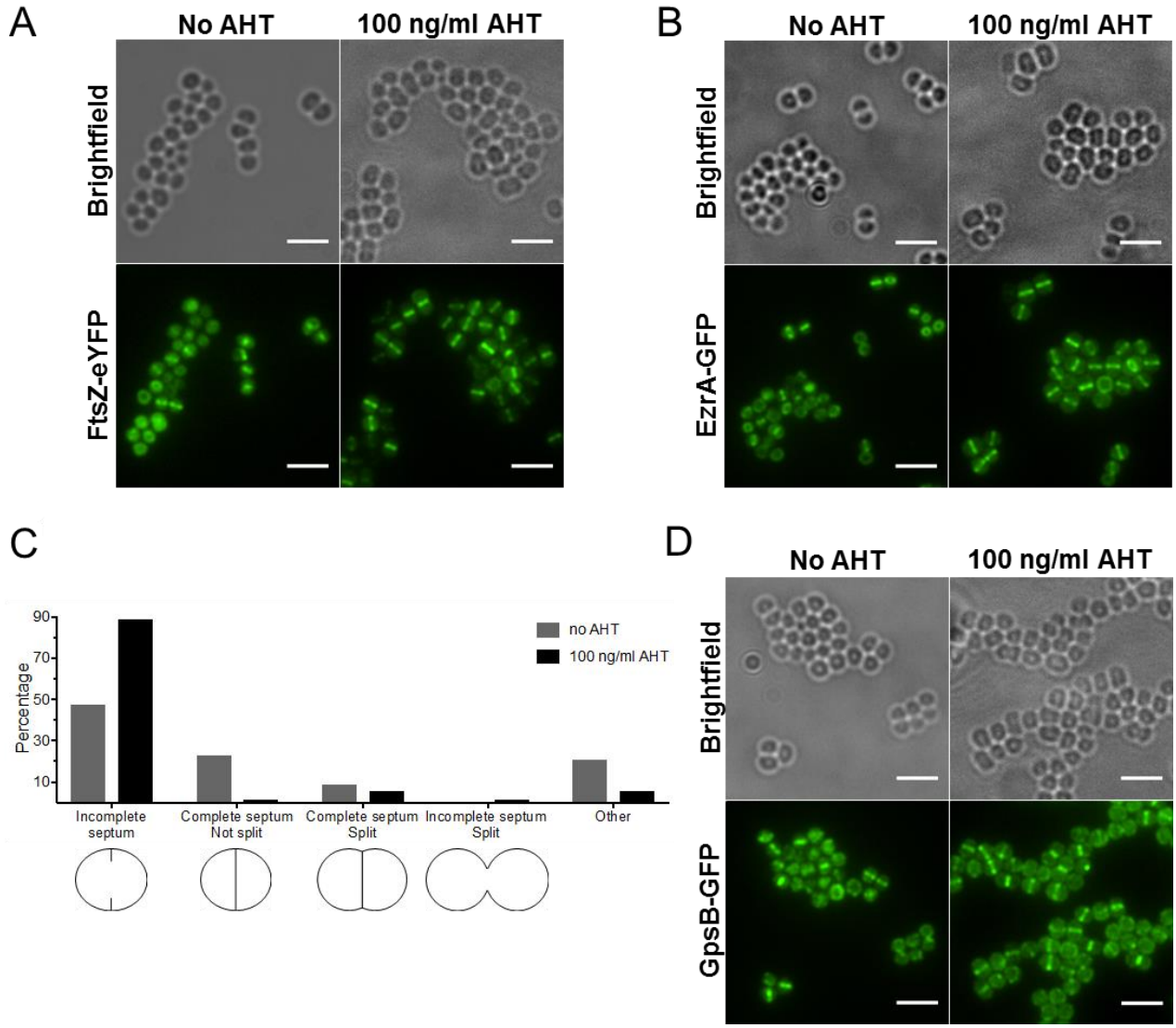

Fig 4 SosA does not impair the localization of cell-division proteins and septum formation initiation. (*A*) Localization of FtsZ-eYFP in SJF4694 (JE2 pSosA pCQ11-FtsZ-eYFP) grown in the absence and presence of 100 ng/ml of AHT for 45 min. (*B*) EzrA-GFP localization in SJF4697 (JE2 pSosA *ezrA-gfp*+) grown in the absence or presence of 100 ng/ml AHT for 45 min. (*C*) Percentages

of JE2 pSosA cells exhibiting incomplete, complete, complete split, or incomplete split septa (n = 573 for no AHT, n = 607 for 100 ng/ml of AHT; organisms either isolated or co-adhered in pairs; other represents staining in indistinct shape) after incubation with or without AHT for 45 min. (*D*) GpsB-GFP localization in SJF700 (JE2 pSosA *gpsB-gfp*+) grown in the absence or presence of 100 ng/ml of AHT for 45 min. All fluorescence images are average intensity projections. All scale bars represent 3 um.

Figure 5

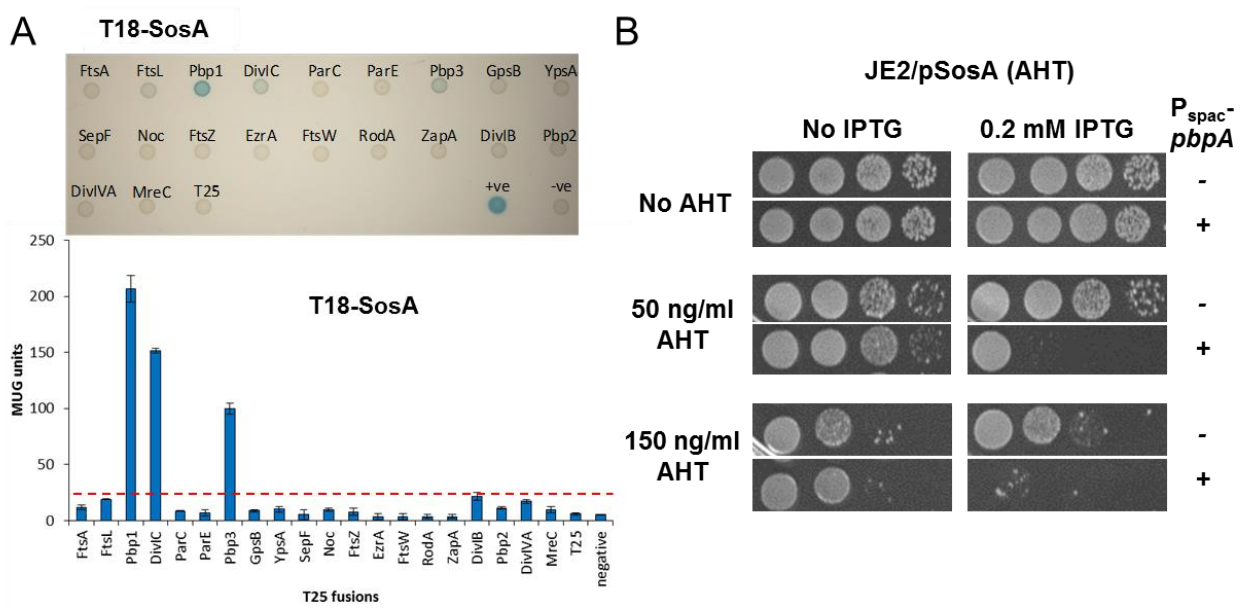

Fig 5 SosA interacts with the central divisome component PBP1. (*A*) Analysis of the protein interactions between SosA and a panel of *S. aureus* cell-division or cell wall-synthesis proteins using the bacterial two-hybrid system. T18 and T25 are domains of an adenylate cyclase enzyme, and the "T18-SosA" and "T25 fusions" labels indicate the fusions between the C-terminus of the T18 adenylate cyclase fragment to the N-terminus of SosA and the T25 fusions to the cell-division proteins. *Top*: Interactions between the *S. aureus* cell-division proteins fused to T25 and *S. aureus*

SosA fused to T18, wherein 10 µl of a 1:100 dilution of overnight culture of co-transformed BTH101 were spotted onto minimal medium containing 150 µg/ml of X-gal and incubated at 30°C for 36 h. +ve, T25-zip + T18-zip; -ve, pKT25 + pUT18C. *Bottom*: β–Galactosidase activity of interactions between *S. aureus* T18-SosA and cell-division proteins (T25 fusions). Activity is displayed as the mean of three independent measurements of β–galactosidase activity, in MUG (4-methylumbelliferyl-β-D-galactopyranoside) units, for each co-transformant. Error bars represent the standard deviation. Positive interactions are considered to be at least four times higher than the activity level for the negative control, and this cut-off level is represented by the red line in the bar chart. (*B*) Assessment of the plating efficiency of *S. aureus* JE2 upon concomitant overexpression of *sosA* (pSosA, AHT-inducible) and *pbpA* (pPBP1) controlled by IPTG (+). (-) denotes the control vector for PBP1. Cells were grown exponentially to an OD_{600} of 0.5, serially 10-fold diluted, and plated on TSA plates containing indicated inducer concentrations. The plates were incubated overnight at 37°C and imaged.

Figure 6

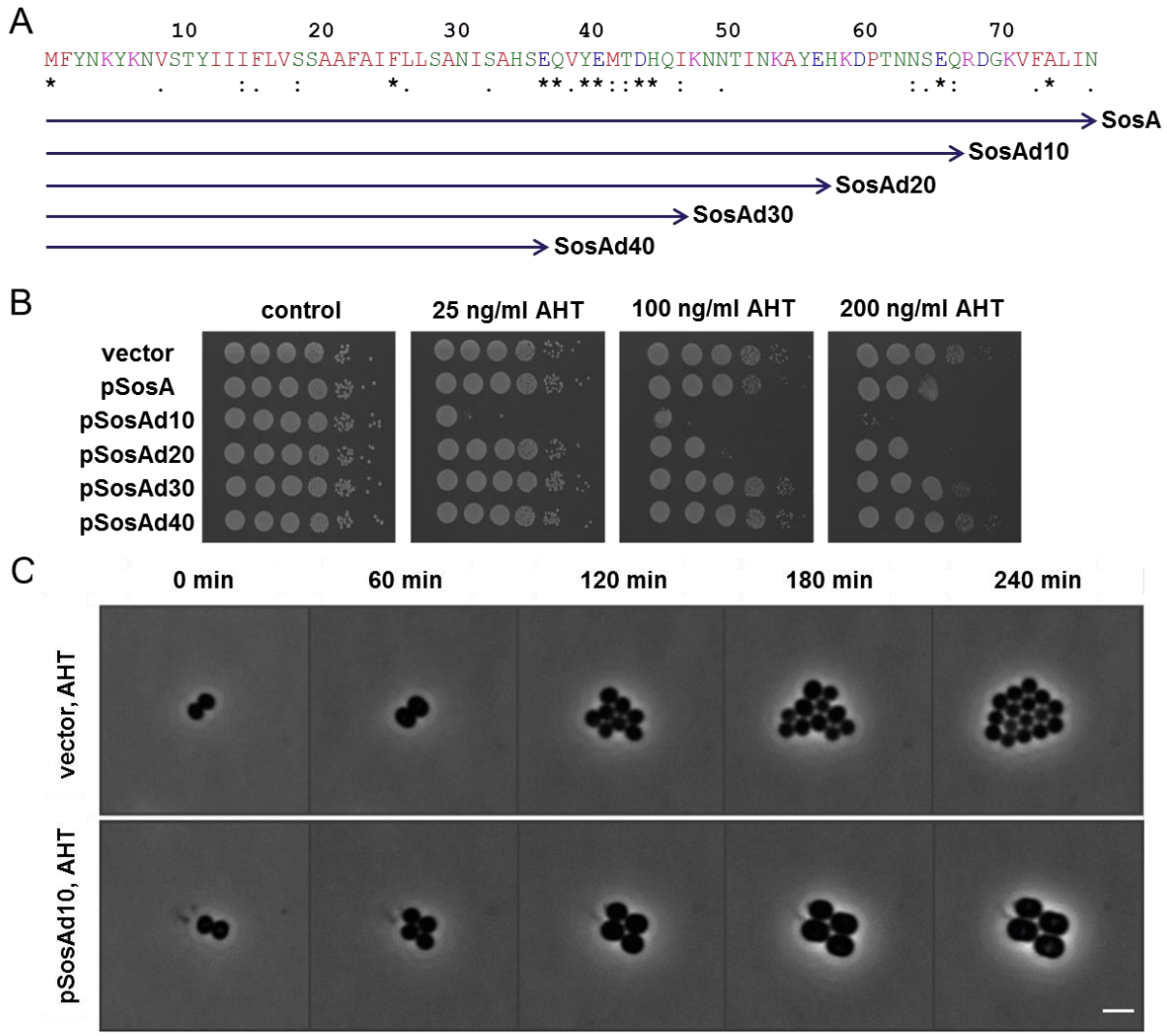

Fig 6 The effect of C-terminal truncations of SosA on the inhibitory activity of the protein. (*A*) Schematic representation of the different truncated SosA constructs. Full-length SosA is a 77-amino-acid peptide. SosAd10 lacks the extreme C-terminal 10 amino acids, while SosAd40 is SosA truncated of almost its entire extracellular C-terminal part. Indicated conserved residues (*****) originate from the alignment in Figure 1. (*B*) Activity of the constructs was assessed in *S. aureus* RN4220 and compared to the vector control (vector). Cells were grown exponentially to an OD_{600} of 0.5, serially 10-fold diluted, and plated on TSA (control) or TSA plus inducer (AHT) at indicated

increasing concentrations followed by incubation overnight at 37°C. (C) Visualization of the drastic cell size increase and the reduction in cell number of JE2/pRAB12-*lacZ* (control) and JE2/pRAB12-*sosAd10* in presence of 200 ng/mL of AHT by time-lapse phase-contrast microscopy at 37°C. Scale bar represents 2 µm.

Figure 7

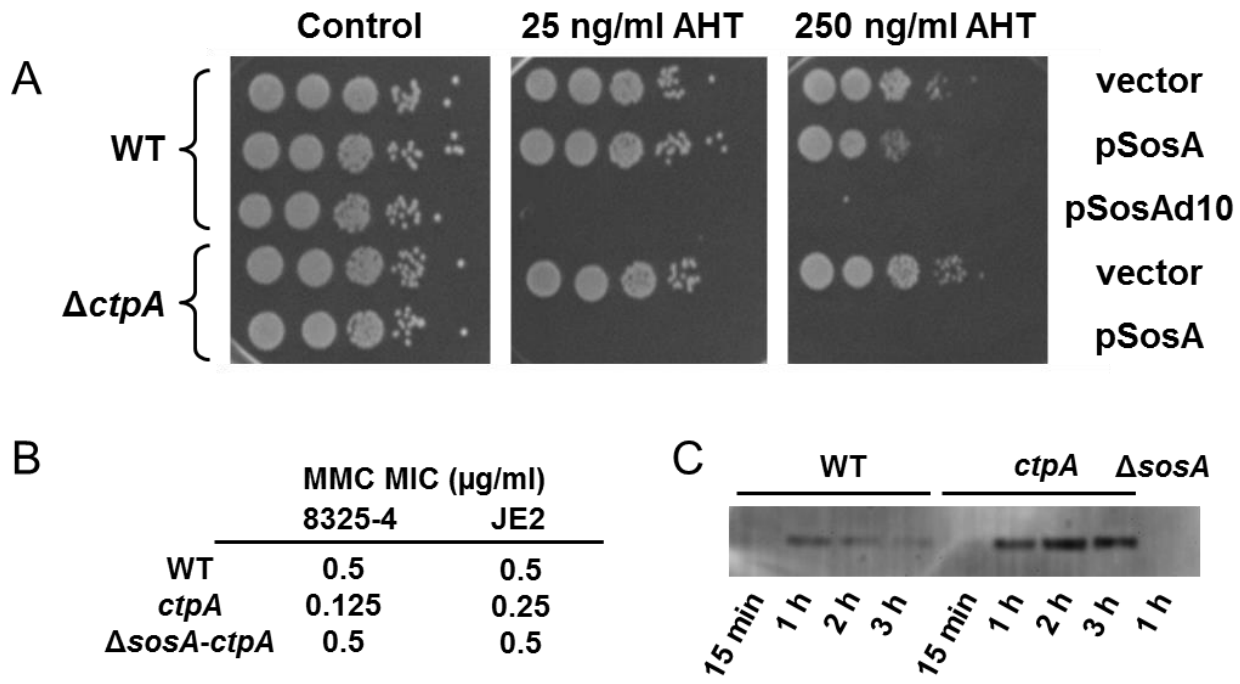

Fig 7 CtpA negatively regulates SosA. (*A*) Hypersusceptibility of an *S. aureus* JE2 *ctpA* mutant to SosA-mediated growth inhibition. Expression of *sosA* (pSosA) in wildtype *S. aureus* JE2 (WT) and the corresponding JE2-*ctpA* mutant (Δ*ctpA*) were compared and referenced to the vector control (vector) and expression of the hyperactive SosAd10 variant (pSosAd10) in the wildtype. Cells were grown exponentially to an OD_{600} of 0.5, serially 10-fold diluted, and plated on TSA (Control) or TSA plus inducer (AHT) at indicated concentrations. The plates were incubated overnight at 37°C and imaged. (*B*) Comparison of mitomycin C (MMC) minimum inhibitory concentration (MIC) for *S.*

aureus 8325-4 and JE2 wildtype, *ctpA*, and Δ*sosA-ctpA* strains. The MICs were obtained by broth dilution. (*C*) Western blot of accumulated SosA in *S. aureus* 8325-4 wildtype (WT) and the *ctpA* mutant at indicated time points after the addition of 0.5 µg/ml of MMC to exponentially growing cells. The *S. aureus* 8325-4Δ*sosA* strain was used as a control.

Figure 8

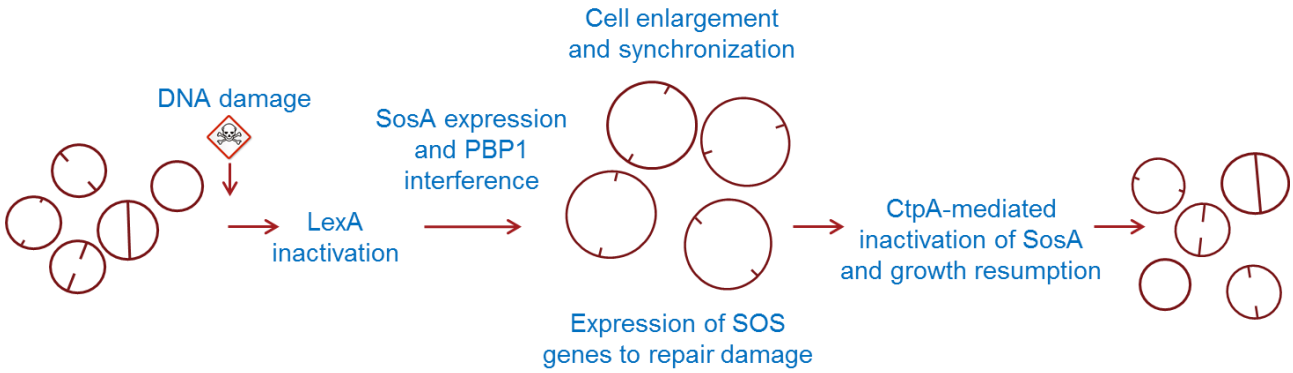

Fig 8 Proposed model for a regulated survival strategy for *S. aureus* upon DNA damage. As part of the SOS response, SosA is produced and, by a membrane-localized activity, corrupts cell-division activity via an interaction with the essential divisome component PBP1. In effect, cells are still able to initiate septum formation but are unable to complete it. This provides a spatio-temporal window for paralleled SOS response-regulated DNA-repair activity. At the same time, the cell size increases due to off-septal activity of peptidoglycan-synthesis enzymes. As the SOS response diminishes, the cellular concentration of SosA is lowered, directly or indirectly, by the proteolytic activity of CtpA. At this stage, septa are allowed to complete and normal growth/division continues.

SI Appendix: 3 supplementary tables, 8 supplementary figures, 3 videos